MICROCOPY   CHART

FOREIGN TECHNOLOGY DIVISION

ACTA OPTICA SINICA

(Selected Articles)

HUMAN TRANSLATION

FTD-ID(RS)T-1089-85   4 April 1986

MICROFICHE NR: FTD-86-C-001693

ACTA OPTICA SINICA (Selected Articles)

English pages: 15

Source: Guangxue Xuebao, Vol. 5, Nr. 2, 1985,
                pp. 117; 157-161

Country of origin: China
Translated by: SCITRAN
                F33657-84-D-0165
Requester: FTD/TQTD
Approved for public release; Distribution unlimited

GRAPHICS DISCLAIMER

All figures, graphics, tables, equations, etc. merged into this
translation were extracted from the best quality copy available.

Accesion For	
NTIS CRA&I	☑
DTIC TAB	☐
Unannounced	☐
Justification	
By	
Distribution /	
Availability Codes	
Dist	Avail and / or Special
A-1	

i

Table of Contents

The Second National Conference On Basic Optics And The Technical
Committee Meeting On Basic Optics Held At Jingbo Lake

The Second National Conference on Basic Optics sponsored by the
Optical Society of China was held July 22-26, 1984 at Jingbo Lake,
Heilongjiang Province, China. About 140 people from 45 institutes of
18 provinces and cities attended the meeting. The meeting featured
150 papers which could be divided into six groups: 1. classical
optics; 2. spectroscopy; 3. high intensity light source and nonlinear
optics effect; 4. optical signal processing and holography; 5.
atmospheric optics; and 6. ocean optics. Some papers from medical
optics were also reported in this meeting.

Since the first National Conference on Basic Optics held in June,
1982, the research works on basic optics in our country had had a lot
of progresses, especially for nonlinear optics, optical signal
processing, and spectroscopy (laser spectroscopy). Among the research
works in nonlinear optics, optical bistability, four-wave mixing, and
stimulated Raman scattering are the three fields which have better
development and almost catch up the level of the well-developed
countries. The optical bistability so far is only on the
demonstration stage in the laboratory. It is still a long way to go
before this technology can be employed for the practical applications.
Similar situation also can be applied to four-wave mixing and
stimulated Raman scattering. For white light signal processing, which
is a very hot topic recently in our country, a lot of scientists and
engineers are doing this kind of research work. So far we have better
understanding on the basic theory of optical signal processing. But

only its encoding method is well developed. In fact, we only follow the other country's direction in this research field. On the other hand, spectroscopy is a tradictional research work in our country and has been studied for a long time. Since the invention of the first laser, laser spectroscopy has been under fully investigation. For the last two decades, we emphasize the atomic laser spectroscopy. Now a lot of research works on molecular laser spectroscopy have been done, which can be seen from the number of papers presented in this meeting.

Comparing with the first meeting, this meeting has some new features. First of all, some papers in the boundary optical science like ocean optics and medical optics were first reported in the meeting. Secondly, young scientists and engineers are the majority among the attendances. More than 20 attendances are graduate students. They reflect the future of the optical technology in our country. Therefore, the overall of this meeting is very exciting and successful.

The Technical Committee Meeting on Basic Optics was also held during the conference. The committee outlined the academic activities for the next 2-3 years. The next conference will be held in 1986.

This conference was co-sponsored by Industry University of Haerbin and by the Insititute of Physics, Academica Sinica.

(Yi Min and Li Chunfei)

The Inhomogeneity of the Optical Thin Film Determined
by Real Time Elliptic Polarization Measurement [++]

Wu Qihong

(Department of Optical Instruments, University of Zhejiang)

ABSTRACT

An automatic photometric ellipsometer with rotating-analyzer is used in our vacuum thin film coater. This ellipsometer can measure the polarization of the depositing thin film instantly. The inhomogeneity of the refractive index can be analyzed from the path curve of the polarization parameters, Δ and Ψ which vary with the thickness of the thin film. The experimental results show that both ZnS and ZnSe have about 100 Å of inhomogeneous transition layers at the inner and outer boundaries. In the central region, it has homogeneous refractive index.

+ Manuscript received March 2, 1984; Revised manuscript received October 5, 1984.

* Supported by Science Foundation of Academica Sinica.

I. Introduction

For the past few decades, the optical thin film had been developed from the simplest single antireflection layer to the modern multilayer stacks of several ten layers. To design and do calculation on these multilayer stacks, an ideal thin film which has the refractive index and geometric thickness as its parameters is usually assumed for the real dielectric thin film. The refractive index of this homogeneous thin film does not change with the increase of its thickness. But a lot of thin films can not be described by this simplified model. Their refractive indices increase or decrease remarkably with increasing the thickness. The inhomogeneity of the refractive index of the oxide thin film is one of the typical examples. The inhomogeneity of the refractive index implies that the microstructure of the thin film may have changed. The dielectric thin film usually has the characteristic of grain-growth. If the grain expands or shrinks with increasing the thin film thickness, the density and then the refractive index of the thin film will also increase or decrease with increasing the thickness. Therefore the study of the inhomogeneity of the thin film refractive index will give the information about the microstructure of the thin film, and is thus a very good subject for further study. There had been some methods used for studying the inhomogeneity of the thin film [2-5]. In this paper, we employ an automatic photometric polarimeter to measure the inhomogeneity of the ZnS, ZnSe, and cryolite thin films which are prepared by the vacuum vaporization method. From these results, the microstructures of the ZnS and ZnSe thin films are estimated.

4

II. Theoretical Analysis and Experimental Method:

It has been known that the ellipsometry has higher sensitivity for the measurements of the dielectric thin film's refractive index and thickness. But the accuracy of the measurement is strongly affected by the inhomogeneity of the thin film's refractive index. A little inhomogeneity in the thin film's refractive index will make the path curve of the polarization parameters Δ and ψ which are functions of the thin film thickness deviate from the homogeneous thin film's path curve. On the other hand, this sensitivity can be used for the measurement of the thin film's inhomogeneity. Since the polarization data can be used to derive the thickness of the thin film, the thickness measurement experiment is not required anymore. This ellipsometry method even can measure the thin film as thin as a few ten of $\overset{\circ}{A}$. Therefore it is better to employ the ellipsometry method for the determination of the inhomogeneity of the thin film's refractive index.

In our experiment, we first measured the thin film at any time during the deposition process by the automatic polarimeter. A large number of the (Δ, ψ) values at different thicknesses of the thin film are obtained. From these data, the path curve of Δ and ψ can be drawn. The inhomogeneity of the refractive index can be roughly determined from this path curve. But the precise values of the refractive index must be determined by using the computer.

It has been known that the curves of equal refractive index of the homogeneous thin film (i.e., the path curves of Δ, ψ)

5

are a series of eggshape closed contours which are not overlapped
with each other.   Each point in the Δ - ψ plane will correspond
to one pair of thin film parameters: refractive index n and
geometric thickness d.

The Δ , ψ path curve of the inhomogeneous thin film is
quite different from that of the homogeneous thin film, i.e., its
(Δ , ψ) is not one to one corresponding to (n, d) anymore. This
is because the changing patterns of the refractive indices may be
different when the thickness starts to increase.

So even for the same (Δ , ψ) point, it may represent different
n and d.   If we compare the path curve of the inhomogeneous thin
film with that of a suitable homogeneous thin film, the changing
pattern of the refractive index of the inhomogeneous thin film
shows some differences which are described below.

According to our calculation, if the refractive index of the
inhomogeneous thin film increases monotonically with the
thickness and is larger than the refractive index of the glass
substrate,   then its path curve (the dot-dash curve in Fig. 1) is
always at the left side of the path curve of the homogeneous thin
film (solid line in Fig. 1) whose refractive index is equal to
the mean refractive index of the inhomogeneous thin film.   If
each   (Δ , ψ) point of this path curve is manipulated according
to the rules of homogeneous thin film, then the calculated
refractive index will not change monotonically with the
thickness.   In this case, if the thickness is less than half
cycle, i.e., at the fourth or the third quadrant of the
coordinate, its refractive index increases with increasing
thickness.   But if the thickness is larger than half cycle, i.e.,

6

at the second or the first quadrant, its refractive index decreases with increasing the thickness. For the case where the refractive index decreases monotonically with increasing the thickness, its path curve (the double-dot dash curve in Fig. 1) is always at the right side of the path curve of the homogeneous thin film whose refractive index is equal to the mean refractive index of the inhomogeneous thin film.

It was found in our experiment that there existed low refractive index transition layers both at the inner and outer boundaries of the thin film. As the thin film thickness increases, the refractive indices and thickness of the inner and outer boundaries almost remain the same. For this kind of inhomogeneous thin film, its path curve at the first half period is at the left side of the path curve of the homogeneous thin film whose refractive index is equal to that of its central region. At the last half period, its path curve shifts to the right side of the path curve of the homogeneous thin film. If every (Δ, ψ) point on this path curve is manipulated according to the rules of the homogeneous thin films, then the calculated refractive indices increase monotonically with increasing the thickness. If the thin film only has the low refractive index inner boundary, its path curve at first is at the left side and then finally merges with the path curve of the homogeneous thin film.

When we analyze the experimental data, we must consider those characteristics we mentioned above for the path curves of the inhomogeneous thin film such that the inhomogeneity of the

7

real thin film can be fully understood.

1. Experimental Set Up

The automatic ellipsometer is chosen here because the thin film refractive index is very sensitive to the variations of the deposition rate, incident angle of vapor, and substrate temperature. In order to reduce the possible uncertainties, the measurements were all done in the vacuum. The automatic ellipsometer is a high speed measuring instrument. For each run, several tens of data points can be obtained. It is therefore possible that the (Δ , ψ) path curve is determined accurately.

Our polarimeter is a RA + FA (rotating-analyzer + fixed-analyzer) type polarimeter. The thin film coater has a cylindrical glass barrel. The light transmits normally through the barrel wall in a horizontal plane. All the optical paths are in the same plane as shown in Fig. 2. The light source is a He-Ne laser with stable power and linear polarization output. The polarization plane of the polarizer is such aligned that it is 45° with respect to the polarization plane of the incident light. So the light incident on the sample has equal amplitude in the P and S components. The sample was clamped vertically in the center of the glass barrel. The deposition source material was also mounted vertically so the vapors would diffuse to the glass substrate horizontally. The laser light, after passing through the barrel wall, was reflected by the sample and passed through an aperture on the barrel wall. When it came out from the barrel, it hit a rotating-analyzer (RA) which is driven by a DC motor. By some photoelectronic techniques, a pulse signal is generated. This signal is used as a synchronous trigger signal.

8

The rotating speed of the analyzer is 40 rpm. For different polarization of the light source, the photomultiplier tube (PMT) has different sensitivity. In order to measure the light intensity accurately, a fixed-analyzer (FA) whose polarization plane is fixed in the X axis is put in between RA and PMT. Our recording system includes an A-D converter and a single-board microprocessor. With this equipment, the light intensity during the deposition process can be collected and analyzed instantly.

According to the theoretical analysis, the light intensity I detected by a detector after it passes through the RA +FA polarimeter can be expressed as a function of polarization angle A of the RA.

$$I = a_0 + a_2 \cos 2A + b_2 \sin 2A + a_4 \cos 4A + b_4 \sin 4A,$$

where a_0, a_2, a_4, b_2, and b_4 are the Fourier coefficients. For each A_i value there is a corresponding I_i value. *If the total number of measurements is N*, then the above Fourier coefficients can be calculated as follows:

$$a_n = \frac{2}{N} \cdot \sum_{i=1}^{N} I_i \cdot \cos nA_i, \quad b_n = \frac{2}{N} \cdot \sum_{i=1}^{N} I_i \cdot \sin nA_i \ .$$

In our case, N could be 20, 36, or even higher number.

From these Fourier coefficients, the Stokes parameters can be derived

$$s_0 = 4 \times (a_0 - a_4), \quad s_1 = \frac{8}{8} \times (a_2 - a_0 + 2a_4), \quad s_2 = \frac{8}{6} \times (2b_2 + b_4)_\circ$$

Finally, Δ and ψ are determined from a simple transformation

$$2\psi = \arccos(-s_1/s_0), \quad \Delta = \arccos(s_2/s_0 \cdot \sin 2\psi)_\circ$$

It should be noted that our polarimeter is not a complete polarimeter. Therefore the Stokes parameter s_3 can not be

9

derived here. Because of this, there is no way to determine if Δ is positive or negative. However, since the thin film is deposited on a blank substrate, the changing trend of the Δ value can be predicted. So unless it is a very special case, there is no problem to determine the sign of Δ .

To do the calculation on the inhomogeneous thin film, the inhomogeneous thin film is replaced by multilayer thin films, where each layer is homogeneous and has a slightly different refractive index compared with other layers. The calculation of the inhomogeneous thin film also can be approximated by using the reflection formula of the multilayer stack in [2].

During the measurement, the glass barrel usually sustains some kind of stress and an extra phase difference of 30°-40° is produced by the double refraction. In order to overcome this problem, every time before we pump the system, we make one measurement without coating on the substrate. This data will be used to adjust the measurement with thin filmson the substrate. Our experiments are done in room temperature, and the vacuum is better than 5×10^{-5} torr. The deposition source material is put very close to the substrate such that the deposition rate is as high as 40 Å/sec. The whole deposition process takes about 60 - 120 sec. The deposition source materials are supplied by Shanhai material refinery.

Three materials are measured in this work; they are ZnS, ZnSe, and Na_3AlF_6. Their experimental curves are shown in Figs. 3, 4, and 5, respectively.

2. Experimental Results

The path curve of the ZnS thin film has the following

10

characteristics.   For each point in the path curve, its
corresponding refractive index of the homogeneous thin film
increases with increasing the thickness (the dot-dash curve in
Fig. 3).   At the first half period, the refractive index is in
between 2.3 and 2.4.   At the last half period, it continues to
increase and has the maximum value of 2.5.   If the inhomogeneity
of the thin film is not taken into consideration, a wrong
conclusion that the refractive index of ZnS is always increasing
smoothly will be made.   As we mentioned before, this kind of path
curve indicates that ZnS has the inner and outer boundaries with
lower refractive indices.   If the change of the refractive index
is due to the change of the density, the refractive indices at
the boundaries should have little change.   From the thin film
charateristics we mentioned above and by using the computer, the
refractive indices which can best fit the experimental data are:
The central region of the ZnS thin film is homogeneous and its
refractive index is 2.36; the thickness of the inner and outer
boundaries is 80 $\overset{c}{A}$ and the refractive index decreases to 2.15.
According to these results, if the total thickness is less than
160 $\overset{c}{A}$, the refractive index in the central region is less than
2.36.   If the total thickness is larger than 160 $\overset{c}{A}$, the
refractive index in the central region is 2.36 even if the thickness
keeps increasing.   But the thickness and the refractive indices
of the inner and outer boundaries remain the same.

The properties of ZnSe are very similar to that of ZnS.
According to the experimental results, the inhomogeneity of the
ZnSe refractive index is also very similar to that of ZnS.   For

11

each point in the ZnSe path curve, its corresponding refractive index of the homogeneous thin film increases smoothly with increasing the thickness (the dot-dash curve in Fig. 4). Similar to ZnS, the best results for ZnSe also can be calculated: The refractive index in the central region of the ZnSe thin film is 2.63; the thickness of the inner and outer boundaries is 120 $\overset{o}{A}$ and their refractive indices decrease to 2.2.

For cryolite, its path curve (see Fig.5) is similar to that of the inhomogeneous thin film whose refractive index decreases monotonically with the thickness. When the thickness of the cryolite thin film is small, for each point of its path curve, the corresponding refractive index of the homogeneous thin film is higher than 1.28. When the thickness reaches 1000 $\overset{o}{A}$, its path curve is very close to the path curve of the homogeneous thin film whose refractive index is equal to 1.28. The cryolite thin film can be approximated by an 800 $\overset{v}{A}$ inhomogeneous layer whose refractive index decreases linearly from 1.34 to 1.28 plus the other inhomogeneous layer (from 800 to 3000 $\overset{o}{A}$) whose refractive index decreases slowly from 1.28 to 1.27. The experimental curve of cryolite is basically consistent with the calculated result of this thin film model. Because cryolite has lower density, its refractive index is lower than that measured in the atmosphere.

III. Discussion

The inhomogeneity of ZnS refractive index had been reported before. The result of Oliver [4] who used the Brewster angle method is that a lower refractive index layer exists in the outer boundary but not in the inner boundary of the ZnS thin film. Netterfield [5], by using the photometric method, found that the

12

refractive index of ZnS thin film increased slowly when its thickness increased from $\lambda/4$ to $\lambda/2$ or even more. By using polarimetric method, King [3] concluded that ZnS had transition layers existing in the inner and outer boundaries. Our observation is consistent with the results of King.

The King's experimental data were obtained from the measurements of a series of discrete samples in the air. However, our data were obtained instantly during the deposition process of the ZnS thin film under the vacuum. We also measured a series of discrete samples by light-attenuated ellipsometer; similar results were obtained (see Table 1). Since there is less interference in the vacuum than in the air, and our results are consistent with each other, it is concluded that the formation of the inhomogeneous surface layer in ZnS is not due to the reaction with the air molecules. Since ZnS and ZnSe have similar structure and inhomogeneity, we think the formation of their inhomogeneous surface layer is due to the change of their microstructure. Based on this assertion we can infer that during the deposition process the atoms must arrive at the substrate at different times. The first few ten $\overset{\circ}{A}$ of the surface layer is thus less crowded and has lower density. The farther away it is from the surface, the more dense it is. This is why the surface boundary becomes inhomogeneous. This mechanism is very similar to the sand pile, where the surface layer is less dense than the central region. In fact, this is only a speculation and more studies are needed in order to prove this hypothesis.
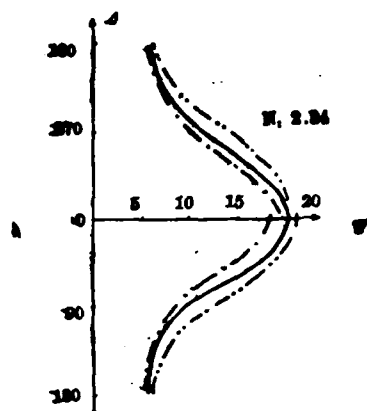
13

Fig. 1 Calculated Δ–Ψ curves of inhomogeneous thin film
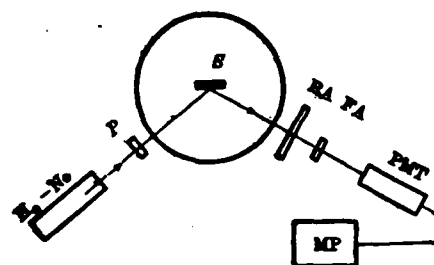
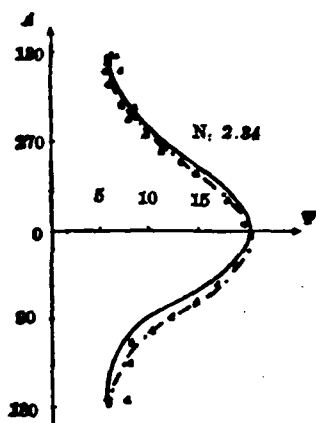Fig. 2 Schematic diagram of RA+FA ellipsometer
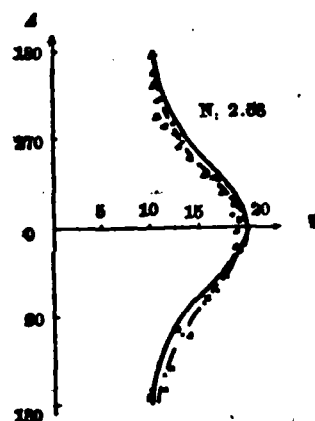

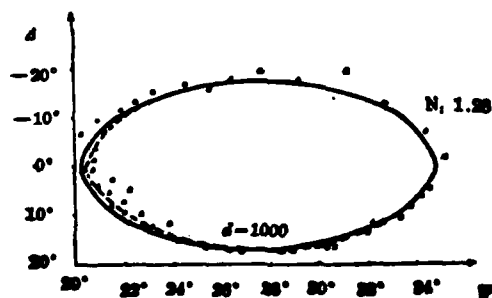Fig. 3 Experimental curve of ZnS

Fig. 4 Experimental curve of ZnSe

Fig. 5 Experimental curve of cryolite

14

REFERENCES

[1] P. S. Haung; *Sur. Sci.*, 1980, 86, No. 1~3 (Jun), 108.
[2] B. Jacobsson; *In Physics of Thin Films*, (Academic Press. Inc New, York), 8, 61.
[3] R. J. King; *Opt. Acta*, 1981, 28, No. 8 (Aug), 1107.
[4] W. B. Oliver; *Opt. Acta*, 1970, 17, No. 8 (Aug), 593.
[5] B. P. Netherfeld; *Appl. Opt.*, 1976, 15, 1960.

Table 1.   Experimental data of discrete sample of ZnS.

	(1) 偏 振 参 数 A, Ψ		(2) 对 应 的 均 匀 膜 n, d	
1	−48.12°	15.70°	2.24	227 Å
2	−52.80°	13.87	2.27	287
3	−61.04	12.55	2.28	333
4	−74.08	10.42	2.29	414
5	−90.2	8.60	2.30	486
6	245.32	6.37	2.31	585
7	223.96	5.38	2.32	645
8	157.42	4.97	2.33	792
9	106.58	7.72	2.34	945
10	83.62	10.87	2.38	1050

Key: 1 - polarization parameter; 2 - corresponding homogeneous
thin film.

15

END

FILMED

5-86

DTIC